

---

# DRAFT

## CMS Physics Analysis Summary

*The content of this note is intended for CMS internal use and distribution only*

---

2013/08/16

Head Id: 202879

Archive Id: 202878:202879M

Archive Date: 2013/08/16

Archive Tag: trunk

### Search for SUSY Partners of Top and Higgs Using Diphoton Higgs Decays

The CMS Collaboration

#### Abstract

We present results of a search for a “natural” SUSY scenario with gauge-mediated breaking. We select events in which there are two photons comprising a Higgs boson candidate, at least two  $b$ -jets and missing transverse energy. Using  $19.5 \text{ fb}^{-1}$  of proton-proton collisions at  $\sqrt{s} = 8 \text{ TeV}$ , recorded in the Compact Muon Solenoid experiment we find no evidence of a signal and set lower limits at the 95% confidence level on the stop mass below 360 to 410 GeV, depending on the higgsino mass.

This box is only visible in draft mode. Please make sure the values below make sense.

PDFAuthor: A. Barker, Y. Gershtein, D. Mason, S. Thomas

PDFTitle: Search for SUSY Partners of Top and Higgs Using Diphoton Higgs Decays

PDFSubject: CMS

PDFKeywords: CMS, physics, SUSY

Please also verify that the abstract does not use any user defined symbols



# 1 Introduction

The recent measurements of the properties of the new boson by ATLAS [1, 2] and CMS [3, 4] confirm that it is likely a Standard Model (SM) Higgs boson. One of the most important problems in particle physics, now that the Higgs boson is established, is to understand why its mass is so small compared to the Planck Scale. Supersymmetry (SUSY) has long offered an elegant solution to this hierarchy problem. Although experimental searches have found no signs of it so far, and the simplest SUSY models become increasingly more constrained, there remain very large yet unprobed areas in SUSY parameter space that would still be “natural”, i.e. have a fairly small amount of fine tuning.

The essential requirement of “natural” SUSY is that the masses of the super-partners of the top quark and the Higgs boson, the stop and the higgsino, are light (see, for example, [5, 6]). In this note we describe a search for events with a topology motivated by SUSY with a Gauge-Mediated SUSY Breaking (GMSB) model [7–10]. We assume a “minimal” number of light SUSY partners, namely right-handed stops and higgsinos. The latter are the lightest chargino ( $\tilde{\chi}_1^+$ ) and neutralinos ( $\tilde{\chi}_1^0, \tilde{\chi}_2^0$ ) and are almost mass-degenerate.

Pairs of higgsinos are produced either directly through electroweak production or through right-handed stop–anti-stop pairs (strong production) with cascade decays

$$\tilde{t}_R \rightarrow b\tilde{\chi}_1^+ \text{ or } t\tilde{\chi}_i^0 \quad (1)$$

where  $i = 1, 2$ . The  $\tilde{\chi}_1^+$  ( $\tilde{\chi}_2^0$ ) subsequently decays into a very off-shell  $W$  ( $Z$ ) boson and a  $\tilde{\chi}_1^0$ . The near mass degeneracy requires the off-shell  $W$  ( $Z$ ) boson decay products to be very soft.

The final decay of the neutralino in all cascades is

$$\tilde{\chi}_1^0 \rightarrow H\tilde{G} \text{ or } Z\tilde{G} \quad (2)$$

Where  $\tilde{G}$  is the gravitino. The branching fractions of  $\tilde{\chi}_1^0$  depend on SUSY parameters. For a significant portion of the parameter space, for example for low values of  $\tan\beta$ , the ratio of the up-type to down-type Higgs vacuum expectation values, and negative values of the supersymmetric Higgs mass term  $\mu$ , Higgs bosons dominate the neutralino decays [11].

The final state we are interested in, therefore, has two  $b$ -jets, two Higgs bosons, and some missing transverse energy from the gravitinos, as shown in Figure 1. In order to suppress SM backgrounds, i.e. from top quark pair production, we take advantage of the known Higgs boson mass and require at least one of the Higgs bosons to decay into two photons. This approach also allows us to use the diphoton mass side-bands for a robust and data driven estimate of background, which is dominated by QCD production of  $\gamma\gamma b\bar{b}$  events and  $\gamma b\bar{b} + j$  events in which the jet is misidentified as a photon.

## 2 Data and Simulation

We use the  $19.5 \text{ fb}^{-1}$  of data collected during the LHC 8 TeV running with the CMS detector, which is described in detail elsewhere [12]. Events are required to pass a suite of diphoton triggers requiring two photon candidates, passing mild shower shape and isolation requirements, with transverse energies above 36 and 22 GeV for the leading and the trailing photon respectively.

We simulate the signal events for a grid of higgsino and stop masses using MADGRAPH 5 v.1.5.4 [13] and PYTHIA 6.4 [14] generators and fast GEANT simulation of the CMS detector [15].

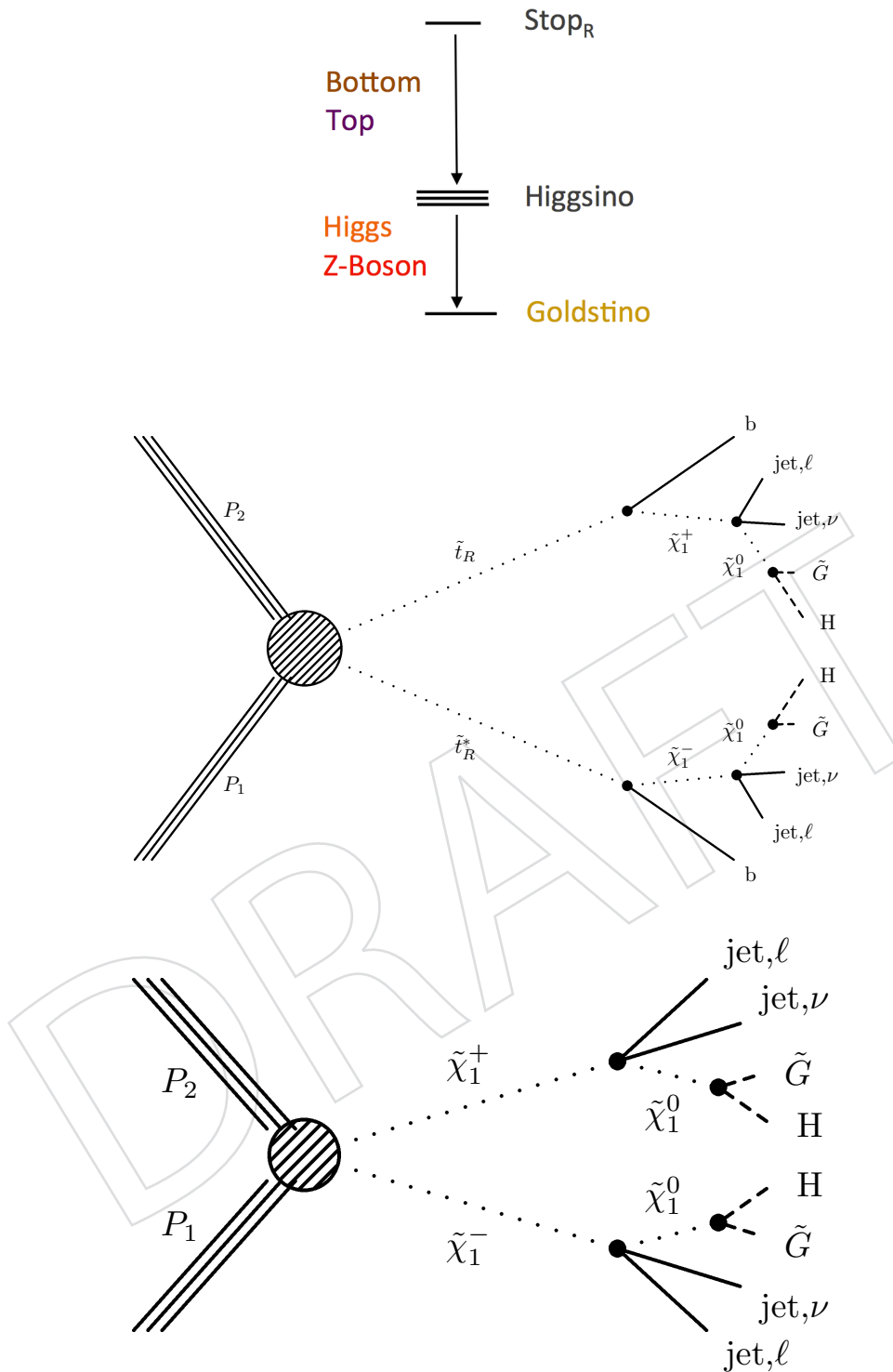


Figure 1: *Top:* The spectrum of the minimal model we consider. *Center:* Example feynman diagram of strong production. *Bottom:* Example feynman diagram of electroweak production. The jets or leptons resulting from transitions between higgsinos are extremely soft in both diagrams due to the near mass degeneracy of the chargino and the neutralino.

37 The next-to-leading order (NLO) cross sections (see Figure 2) are calculated using PROSPINO [16–  
 38 20]. We set the higgsino mass splittings to 5 GeV, and use 100% branching fraction for  $\tilde{\chi}_1^0 \rightarrow H\tilde{G}$  decay.

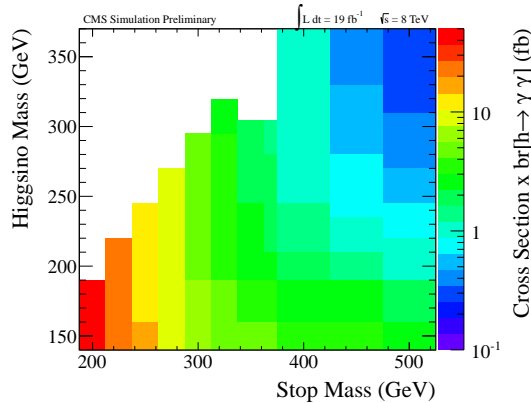


Figure 2: Cross section  $\times br[h \rightarrow \gamma\gamma]$  for the generated MC points.

39

### 40 3 Object Reconstruction and Identification

41 Photon candidates are reconstructed from the energy deposits in the ECAL, grouping its channels  
 42 into a supercluster [21]. We require photons to register in the barrel portion of the calor-  
 43 imeter ( $|\eta| < 1.4442$ ) and pass shower shape and isolation requirements. To reject electrons  
 44 misidentified as photons, we also require that photons do not have associated hit patterns in  
 45 the pixel detector consistent with a track. Photon energies are calculated using multivariate  
 46 regression following the method described in reference [22].

47 We use the particle flow (PF) algorithm [23] to reconstruct individual particles in the events,  
 48 combining all available sub-detector information in a coherent and optimal manner. Jets are  
 49 reconstructed from the PF particles using the anti- $k_T$  [24] algorithm. The two leading identified  
 50 photons are removed from the jet list using a  $\Delta R$  cut of 0.6 and a  $\Delta\phi$  cut of 0.05 radians. We  
 51 apply  $p_T$ - and  $\eta$ -dependent corrections to the jet energies to account for residual effects of non-  
 52 uniform detector response. The pileup contribution is estimated and subtracted from the jet  
 53 energy using the jet area method [25] on an event-by-event basis. The combined secondary  
 54 vertex (CSV) algorithm [26] is employed to identify jets that come from a b-quark.

55 The missing transverse energy ( $E_T^{\text{miss}}$ ) in the event is computed as minus the vectorial sum  
 56 of the transverse momenta of all PF candidates [23]. We also calculate the following event  
 57 kinematics variables:

- 58 •  $H_T$ : the scalar sum of the  $p_T$  of all the jets in the event,
- 59 •  $B_T$ : the scalar sum of the  $p_T$  of all the CSV-LOOSE  $b$ -jets in the event,
- 60 •  $S_T$ : the scalar sum of the  $E_T^{\text{miss}}$ , the  $H_T$ , and the  $p_T$  of photon candidates,
- 61 •  $H_T^{\text{miss}}$ : the vectorial sum of the  $p_T$  of all the jets in the event.

## 4 Event Selection and Categorization

The events are selected if they have at least two identified photons, with transverse energies above 40 and 25 GeV for the leading and trailing photons respectively. Events are also required to have at least two jets with transverse energy above 30 GeV and  $|\eta| < 2.4$  and pass the CSV-LOOSE requirements, and at least one of which also must pass the CSV-MEDIUM requirement.

The events with diphoton mass between 120 and 131 GeV constitute the *signal sample*, while the events with mass between 103 and 118 GeV and between 133 and 163 GeV comprise the *lower side-band* and *upper side-band* samples respectively.

The SUSY events we look for have multiple  $b$ -jets. The dominant decay of the Higgs boson is to  $b$ -quarks, and, in case of strong production, one expects two more  $b$ -jets from the stop to higgsino decay. We exploit this by separating events into three categories as follows:

1. events with at least one additional CSV-LOOSE  $b$ -jet in addition to the two (i.e. events with three or more  $b$ -jets)
2. events for which the invariant mass of the two  $b$ -jets is within a Higgs mass window, from 95 to 155 GeV
3. all other events.

The distribution of signal events between the three categories depends on the stop and higgsino masses. For small mass differences between the stop and the higgsino, most of the signal populates category 2, while for large mass differences categories 1 and 3 dominate.

The search is performed independently in the three categories and the results are combined, leading to up to a 35% increase in expected SUSY cross-section limits compared to the analysis without categorization.

## 5 Background Prediction

The background from standard model Higgs production was found to be negligible for this analysis in Monte Carlo simulations. We use sidebands around the Higgs mass in the diphoton mass distribution to derive a robust data driven measure of all non-Higgs standard model background processes. The background predictions are shown in Figure 3 and 4 as the red thatched rectangles.

The background is dominated by QCD production of  $\gamma\gamma b\bar{b}$  events and  $\gamma b\bar{b} + j$  events in which a jet is misidentified as a photon. We measured the component of the background due to electrons misidentified as photon in data and found that this is a minute contribution. In any case, the sideband method allows us to accurately determine the standard model background regardless of its composition.

We divide the diphoton mass distribution into three regions: a narrow signal region on the Higgs mass and two sidebands on either side of it, with 2 GeV buffer regions in between. We fit the diphoton distribution using a power law from 105-160 GeV. The region from 118-133 GeV, corresponding to the signal region plus the buffers, is excluded from the fitter's consideration to prevent potential signal from affecting the background estimate. The fit function is used to determine the normalization of the background. We explored the effects of various other fit

101 functions and resulting variations in the fit function integrals are well described by the uncer-  
 102 tainty in the fit function integral by from the power law fit.

103 We then make distributions of our kinematic variables of interest for both the upper and lower  
 104 sidebands. This gives us two independent estimates for the distributions of the standard model  
 105 background. In determining the uncertainty in each of these estimates we take into account the  
 106 statistical correlation between the content of each bin and the entire sideband.

107 The amount of standard model background is guaranteed to be somewhere between the esti-  
 108 mates of the upper and lower side band. In principal there may be correlations between the  
 109 diphoton mass and other kinematic variables. We form our main background estimate by tak-  
 110 ing the bin-by-bin average of the two background estimates from the side bands. We take half  
 111 the difference, bin-by-bin, between the two estimates as a systematic uncertainty so that the  
 112 uncertainty in the main background estimate spans the difference between the two estimates.  
 113 For  $E_T^{\text{miss}}$  the uncertainty is statistics limited and the systematic uncertainty is relatively unim-  
 114 portant.

115 In determining the uncertainty on the main background estimate, and in limit setting, we take  
 116 into account that the same fit function and it's uncertainty are used for both estimates and for  
 117 every bin in the histogram.

## 118 6 Results

119 The observed distributions of  $E_T^{\text{miss}}$  are shown in Figure 3 separately for the three event cate-  
 120 gories, and for the entire dataset, together with the data-driven background expectation and  
 121 the expected distributions for three signal mass points. Figure 4 shows the distributions of  
 122  $H_T$ ,  $S_T$ ,  $B_T$ , and  $H_T^{\text{miss}}$  for the data, the background predictions, and representative signal mass  
 123 points. These four variables and  $E_T^{\text{miss}}$  have somewhat complementary sensitivity, as can be  
 124 seen in the relative differences between the distributions of predicted background and that of  
 125 signal for the three mass points.

126 Table 1 shows the total event counts, the total background predictions, and expected signal  
 127 yields, for the three event categories. The background estimates for each category are from the  
 128 power-law fits to the diphoton mass ( $M_{\gamma\gamma}$ ) distributions in the corresponding category. The  
 129 uncertainties on the background estimates here are due entirely to uncertainties in the integrals  
 130 of the fit functions. The observations are in agreement with the background predictions.

Table 1: Expected and observed event counts. The yields for three signal points are show for comparison indicating  $M_{\text{stop}}$  and  $M_{\text{higgsino}}$  respectively.

	On $H$ mass	Off $H$ mass	3 + $b$ -jets
signal 350 / 135 GeV	2.0	6.8	10.7
signal 300 / 290 GeV	10.1	3.9	2.1
signal 400 / 300 GeV	1.4	2.8	4.0
expected BG	$10.8 \pm 2.1$	$28.7 \pm 3.0$	$6.3 \pm 1.5$
observed	7	33	6

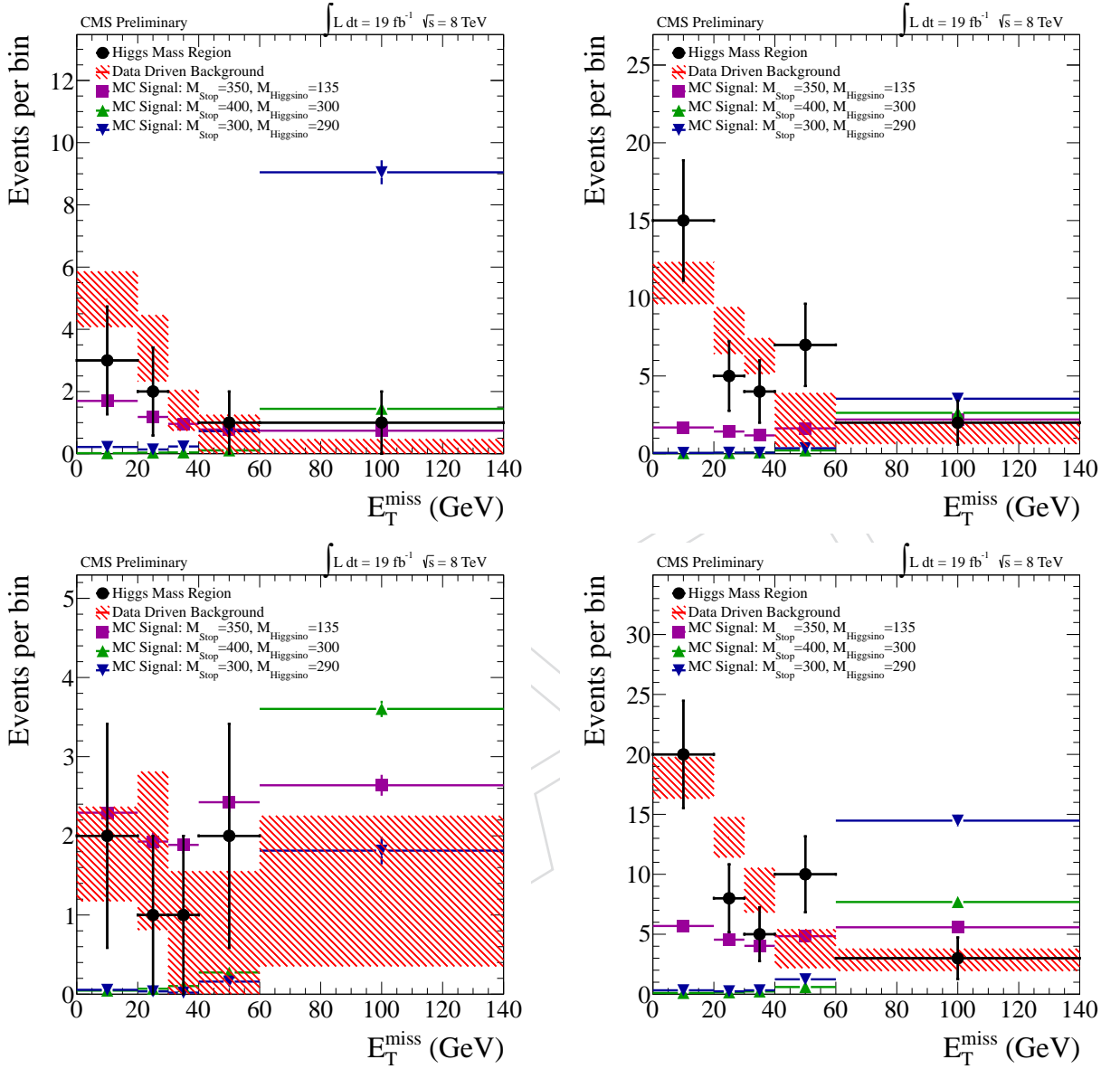


Figure 3:  $E_T^{\text{miss}}$  distributions for the data, background predictions, and representative signals for the three  $b$ -jet categories (see Section 4). Upper left: the 2  $b$ -jets category with  $M_{bb}$  on the Higgs mass. Upper Right: the 2  $b$ -jets category with  $M_{bb}$  off the Higgs mass. Lower left: the 3 or more  $b$ -jets category. Lower right: the sum of the three categories. Signal point masses are in units of GeV. For each histogram, the last bin includes the overflow. The first three plots hold all the data and background estimates used for limit setting.

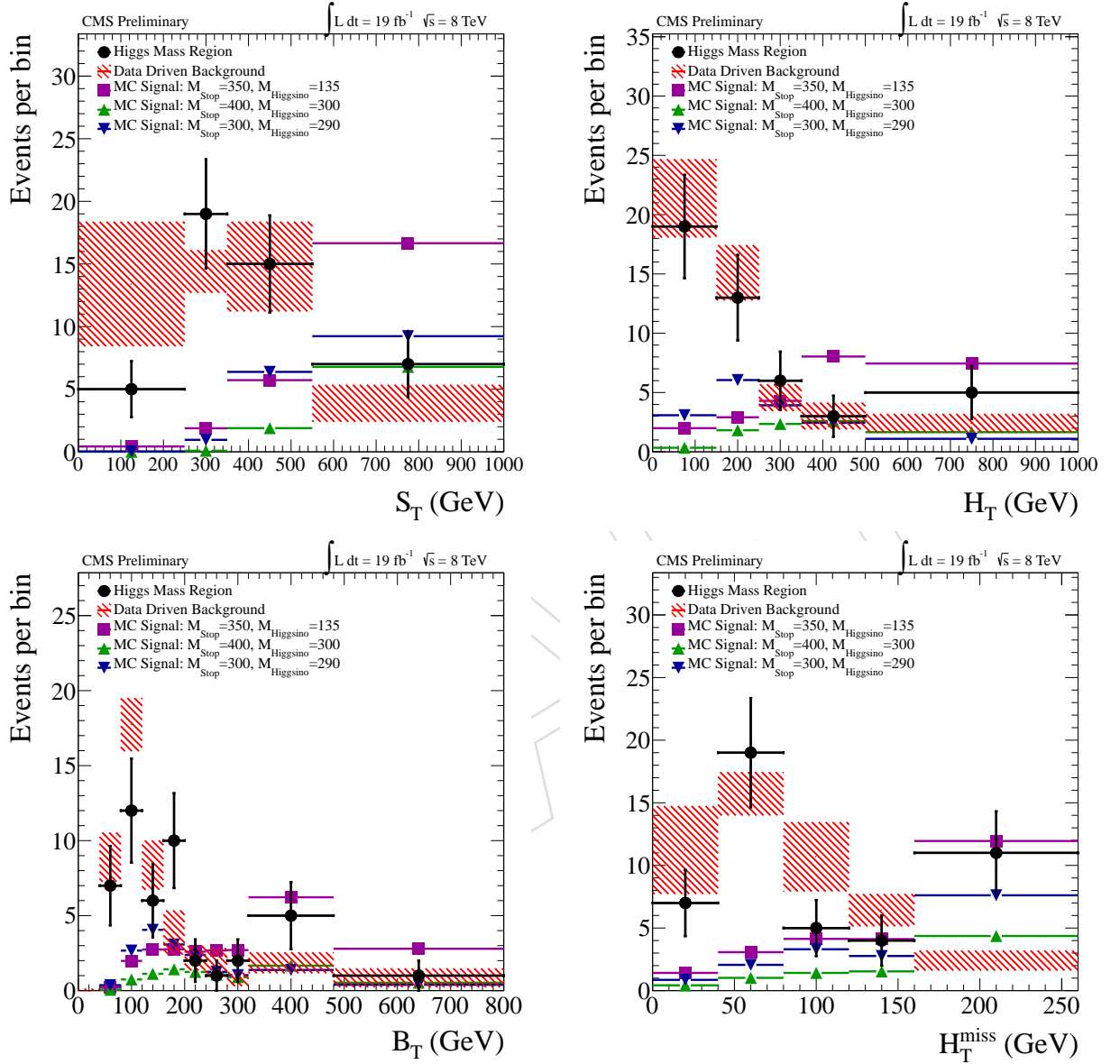


Figure 4: The distributions of  $H_T$ ,  $S_T$ ,  $B_T$  and  $H_T^{miss}$  for the data, background predictions (shaded rectangles), and selected Monte Carlo mass points (color points). For each histogram, the last bin includes the overflow.

## 7 Statistical Interpretation

Since the data agree with the expected background we proceed to set limits on the signal model. We calculated the expected limits using a variety of kinematic variables and determined that  $E_T^{\text{miss}}$  is the single most sensitive variable. The observed  $E_T^{\text{miss}}$  distributions for the three  $b$ -jet categories, shown in Figure 3, together with the signal and background expectations listed in Table 1, are used as input to the limit-setting.

We use an LHC-style profiled likelihood test statistics using the "Asymptotic CLs" method [27]. For each model mass point, the modified frequentist  $CL_S$  criterion [28, 29] is used to calculate upper limits on the cross section for the model.

The dominant uncertainty in the analysis is the statistical uncertainty of the background prediction. The sources of systematics on the signal include the uncertainties in integrated luminosity [30], the diphoton trigger efficiency, the photon reconstruction and identification efficiency, the photon resolution uncertainty, the jet energy scale, and the  $b$ -jet identification efficiency. All systematic uncertainties are correlated between the  $b$ -jet categories and are treated as nuisance parameters in the likelihood, profiled according to their estimated value (see Table 2).

Figure 5 shows the limits we obtain for the GMSB model in the stop-higgsino mass plane. Depending on the higgsino mass, we are able to exclude stop masses below 360 to 400 GeV with 95% confidence, corresponding to the region to the left of the thick black line in Figure 5.

Table 2: Sources of systematic uncertainties

Source of Uncertainty	Value
Trigger efficiency uncertainty	0.1%
Photon efficiency uncertainty	1%
Photon resolution uncertainty	1%
B-jet identification uncertainty	shape uncertainty: 1-5% for 2 B-jets, 6-17% for 3 B-jets
Jet energy scale uncertainty	shape uncertainty 7-43% for $20 < E_T^{\text{miss}} < 40$ GeV; negligible elsewhere
Luminosity uncertainty	4.4%
Signal theoretical cross-section uncertainty	$\sim 15\%$ [31]

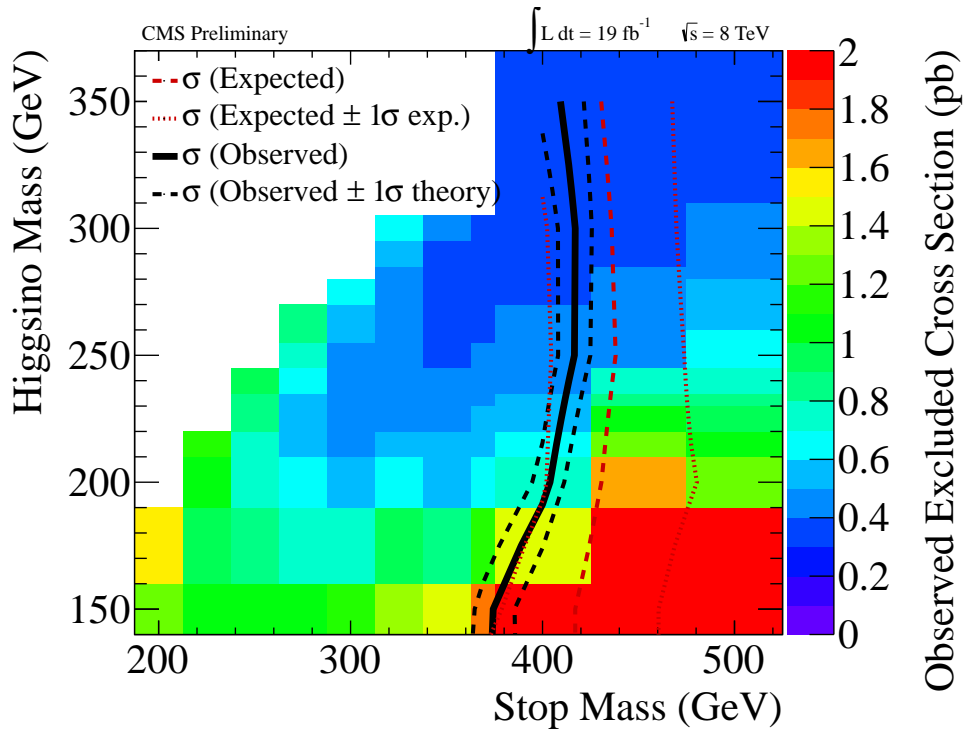


Figure 5: Limit on the stop pair production cross section using  $b$ -jet categories. The regions to the left of the contours are expected (red) and observed (black) to be excluded with 95% confidence.

## 149 8 Conclusion

150 We have performed a search for a “natural” SUSY scenario with light higgsinos and a stop  
 151 using Higgs tagging in the diphoton decay mode in a final state containing at least two photons,  
 152 two or more  $b$ -jets, and missing transverse energy. No evidence for a signal is observed, and  
 153 95% CL limits are set in the stop - higgsino mass plane, excluding a significant portion of the  
 154 “natural” parameter space up to stop masses of 400 GeV.

## References

- [1] “Study of the spin of the new boson with up to  $25 \text{ fb}^{-1}$  of ATLAS data”, Technical Report ATLAS-CONF-2013-040, CERN, Geneva, (Apr, 2013).
- [2] “Combined coupling measurements of the Higgs-like boson with the ATLAS detector using up to  $25 \text{ fb}^{-1}$  of proton-proton collision data”, Technical Report ATLAS-CONF-2013-034, CERN, Geneva, (Mar, 2013).
- [3] CMS Collaboration Collaboration, “Study of the Mass and Spin-Parity of the Higgs Boson Candidate Via Its Decays to Z Boson Pairs”, *Phys.Rev.Lett.* **110** (2013) 081803, doi:10.1103/PhysRevLett.110.081803, arXiv:1212.6639.
- [4] “Properties of the observed Higgs-like resonance using the diphoton channel”, Technical Report CMS-PAS-HIG-13-016, CERN, Geneva, (2013).
- [5] R. Barbieri and G. Giudice, “Upper Bounds on Supersymmetric Particle Masses”, *Nucl.Phys.* **B306** (1988) 63, doi:10.1016/0550-3213(88)90171-X.
- [6] M. Papucci, J. T. Ruderman, and A. Weiler, “Natural SUSY Endures”, *JHEP* **1209** (2012) 035, doi:10.1007/JHEP09(2012)035, arXiv:1110.6926.
- [7] S. Dimopoulos et al., “Experimental signatures of low-energy gauge mediated supersymmetry breaking”, *Phys.Rev.Lett.* **76** (1996) 3494–3497, doi:10.1103/PhysRevLett.76.3494, arXiv:hep-ph/9601367.
- [8] S. Ambrosanio et al., “Search for supersymmetry with a light gravitino at the Fermilab Tevatron and CERN LEP colliders”, *Phys.Rev.* **D54** (1996) 5395–5411, doi:10.1103/PhysRevD.54.5395, arXiv:hep-ph/9605398.
- [9] K. T. Matchev and S. D. Thomas, “Higgs and Z boson signatures of supersymmetry”, *Phys.Rev.* **D62** (2000) 077702, doi:10.1103/PhysRevD.62.077702, arXiv:hep-ph/9908482.
- [10] K. Howe and P. Saraswat, “Excess Higgs Production in Neutralino Decays”, *JHEP* **1210** (2012) 065, doi:10.1007/JHEP10(2012)065, arXiv:1208.1542.
- [11] P. Meade, M. Reece, and D. Shih, “Prompt Decays of General Neutralino NLSPs at the Tevatron”, *JHEP* **1005** (2010) 105, doi:10.1007/JHEP05(2010)105, arXiv:0911.4130.
- [12] CMS Collaboration, “The CMS experiment at the CERN LHC”, *JINST* **3** (2008) S08004, doi:10.1088/1748-0221/3/08/S08004.
- [13] J. Alwall et al., “MadGraph 5 : Going Beyond”, *JHEP* **1106** (2011) 128, doi:10.1007/JHEP06(2011)128, arXiv:1106.0522.
- [14] T. Sjöstrand, S. Mrenna, and P. Skands, “PYTHIA 6.4 physics and manual”, *JHEP* **05** (2006) 026, doi:10.1088/1126-6708/2006/05/026, arXiv:hep-ph/0603175.
- [15] “CMS Physics: Technical Design Report Volume 1: Detector Performance and Software”. Technical Design Report CMS. CERN, Geneva, 2006.

- 192 [16] W. Beenakker et al., “Squark and gluino production at hadron colliders”, *Nucl.Phys.*  
193 **B492** (1997) 51–103, doi:10.1016/S0550-3213(97)80027-2,  
194 arXiv:hep-ph/9610490.
- 195 [17] A. Kulesza and L. Motyka, “Threshold resummation for squark-antisquark and  
196 gluino-pair production at the LHC”, *Phys.Rev.Lett.* **102** (2009) 111802,  
197 doi:10.1103/PhysRevLett.102.111802, arXiv:0807.2405.
- 198 [18] W. Beenakker et al., “Soft-gluon resummation for squark and gluino hadroproduction”,  
199 *JHEP* **0912** (2009) 041, doi:10.1088/1126-6708/2009/12/041,  
200 arXiv:0909.4418.
- 201 [19] W. Beenakker et al., “Squark and Gluino Hadroproduction”, *Int.J.Mod.Phys.* **A26** (2011)  
202 2637–2664, doi:10.1142/S0217751X11053560, arXiv:1105.1110.
- 203 [20] W. Beenakker, R. Hopker, and M. Spira, “PROSPINO: A Program for the production of  
204 supersymmetric particles in next-to-leading order QCD”, arXiv:hep-ph/9611232.
- 205 [21] “Photon reconstruction and identification at sqrt(s) = 7 TeV”, Technical Report  
206 CMS-PAS-EGM-10-005, CERN, 2010. Geneva, (2010).
- 207 [22] “Updated measurements of the Higgs boson at 125 GeV in the two photon decay  
208 channel”, Technical Report CMS-PAS-HIG-13-001, CERN, Geneva, (2013).
- 209 [23] CMS Collaboration, “Commissioning of the Particle-Flow Reconstruction in  
210 Minimum-Bias and Jet Events from pp Collisions at 7 TeV”, *CMS PAS PFT-10-002* (2010).
- 211 [24] M. Cacciari, G. P. Salam, and G. Soyez, “The anti- $k_t$  jet clustering algorithm”, *JHEP* **04**  
212 (2008) 063, doi:10.1088/1126-6708/2008/04/063, arXiv:0802.1189.
- 213 [25] M. Cacciari and G. P. Salam, “Pileup subtraction using jet areas”, *Physics Letters B* **659**  
214 (2008), no. 12, 119 – 126,  
215 doi:http://dx.doi.org/10.1016/j.physletb.2007.09.077.
- 216 [26] CMS Collaboration, “b-Jet Identification in the CMS Experiment”, *CMS PAS BTV-11-004*  
217 (2011).
- 218 [27] ATLAS and CMS Collaborations, LHC Higgs Combination Group, “Procedure for the  
219 LHC Higgs boson search combination in Summer 2011”, *ATL-PHYS-PUB/CMS NOTE*  
220 2011-11, 2011/005, (2011).
- 221 [28] T. Junk, “Confidence level computation for combining searches with small statistics”,  
222 *Nucl. Instrum. Meth. A* **434** (1999) 435, doi:10.1016/S0168-9002(99)00498-2,  
223 arXiv:hep-ex/9902006.
- 224 [29] A. L. Read, “Presentation of search results: The CL(s) technique”, *J. Phys. G* **28** (2002)  
225 2693, doi:10.1088/0954-3899/28/10/313.
- 226 [30] CMS Collaboration, “CMS Luminosity Based on Pixel Cluster Counting - Summer 2012  
227 Update”, Technical Report CDS Record 1482193, (2012).
- 228 [31] M. Kramer et al., “Supersymmetry production cross sections in  $pp$  collisions at  $\sqrt{s} = 7$   
229 TeV”, arXiv:1206.2892.